DEUTSCHES ELEKTRONEN – SYNCHROTRON

DESY

DESY 92-040
March 1992

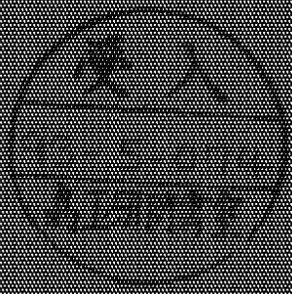

Observation of Two-Jet Production in Deep Inelastic Scattering at HERA

ZEUS Collaboration

ISSN 0418-9833

NOTKESTRASSE 85 – D-2000 HAMBURG 52

DESY 93-030
March 1993

ISSN 0418-9833

Observation of two-jet production in deep inelastic scattering at HERA

ZEUS Collaboration

16 March 1993

Abstract

A sample of events with two distinct jets, in addition to the proton remnant, has been identified in deep inelastic, neutral current *ep* interactions recorded at HERA by the ZEUS experiment. For these events, the mass of the hadronic system ranges from 40 to 260 GeV. The salient features of the observed jet production agree with the predictions of higher order QCD.

The ZEUS Collaboration

M. Derrick, D. Krakauer, S. Magill, B. Musgrave, J. Repond, S. Repond, R. Stanek, R.L. Talaga, J. Thron
Argonne National Laboratory, Argonne, IL, USA

F. Arzarello, R. Ayad[1], G. Bari, M. Basile, L. Bellagamba, D. Boscherini, A. Bruni, G. Bruni, P. Bruni, G. Cara Romeo, G. Castellini [2], M. Chiarini, L. Cifarelli, F. Cindolo, F. Ciralli, A. Contin, S. D'Auria, C. Del Papa, F. Frasconi, P. Giusti, G. Iacobucci, G. Laurenti, G. Levi, Q. Lin,B. Lisowski, G. Maccarrone, A. Margotti, T. Massam, R. Nania, C. Nemoz, F. Palmonari, G. Sartorelli, R. Timellini, Y. Zamora Garcia[1], A. Zichichi
University and INFN Bologna, Bologna, Italy

A. Bargende, J. Crittenden, H. Dabbous[3], K. Desch, B. Diekmann, T. Doeker, M. Geerts, G. Geitz, B. Gutjahr, H. Hartmann, D. Haun, K. Heinloth, E. Hilger, H.-P. Jakob, S. Kramarczyk, M. Kückes, A. Mass, S. Mengel, J. Molten, D. Monaldi, H. Müsch, E. Paul, R. Schattevoy, J.-L. Schneider, R. Wedemeyer
Physikalisches Institut der Universität Bonn, Bonn, Federal Republic of Germany

A. Cassidy, D.G. Cussans, N. Dyce, H.F. Fawcett, B. Foster, R. Gilmore, G.P. Heath, M. Lancaster, T.J. Llewellyn, J. Malos, C.J.S. Morgado, R.J. Tapper, S.S. Wilson
Bristol University, Bristol, U.K.

R.R. Rau
Brookhaven National Laboratory, Upton, L.I., USA

M. Arneodo, T. Barillari, M. Schioppa, G. Susinno
Calabria University, Physics Dept.and INFN, Cosenza, Italy

A. Bernstein, A. Caldwell, I. Gialas, J.A. Parsons, S. Ritz, F. Sciulli[4], P.B. Straub, L. Wai, S. Yang
Columbia University, Nevis Labs., Irvington on Hudson,N.Y., USA

J. Chwastowski[5], A. Dwurażny, A. Eskreys, Z. Jakubowski[6], B. Nizioł, K. Piotrzkowski, M. Zachara, L. Zawiejski
Inst. of Nuclear Physics, Cracow, Poland

B. Bednarek, P. Borzemski, K. Eskreys, K. Jeleń, D. Kisielewska, T. Kowalski, E. Rulikowska-Zarębska, L. Suszycki, J. Zając
Faculty of Physics and Nuclear Techniques, Academy of Mining and Metallurgy, Cracow, Poland

T. Kędzierski, A. Kotański, M. Przybycień
Jagellonian Univ., Dept. of Physics, Cracow, Poland

L.A.T. Bauerdick, U. Behrens, J.K. Bienlein, C. Coldewey, A. Dannemann, G. Drews, P. Erhard[7], M. Flasiński[8], I. Fleck, R. Gläser[9], P. Göttlicher, T. Haas, L. Hagge, W. Hain, D. Hasell, H. Hultschig, G. Jahnen[10], P. Joos, M. Kasemann, R. Klanner, W. Koch, U. Kötz, H. Kowalski, J. Krüger, J. Labs, A. Ladage, B. Löhr, M. Löwe, D. Lüke, J. Mainusch, O. Manczak[11], M. Momayezi, J.S.T. Ng, S. Nickel, D. Notz, I.H. Park, K.-U. Pösnecker[12], M. Rohde, J. Roldán[13], E. Ros[5], U. Schneekloth, J. Schroeder, W. Schulz, F. Selonke, E. Stiliaris[13], E. Tscheslog[14], T. Tsurugai, F. Turkot[15], W. Vogel[16], G. Wolf, C. Youngman
Deutsches Elektronen-Synchrotron DESY, Hamburg, Federal Republic of Germany

H.J. Grabosch, A. Leich, A. Meyer, C. Rethfeldt, S. Schlenstedt
DESY-Zeuthen, Inst. für Hochenergiephysik, Zeuthen, Federal Republic of Germany

G. Barbagli, A. Francescato, M. Nuti, P. Pelfer
University and INFN, Florence, Italy

G. Anzivino, R. Casaccia, S. De Pasquale, S. Qian, L. Votano
INFN, Laboratori Nazionali di Frascati, Frascati, Italy

A. Bamberger, A. Freidhof, T. Poser, S. Söldner-Rembold, G. Theisen, T. Trefzger
Physikalisches Institut der Universität Freiburg, Freiburg, Federal Republic of Germany

N.H. Brook, P.J. Bussey, A.T. Doyle, J.R. Forbes, V.A. Jamieson, C. Raine, D.H. Saxon
Dept. of Physics and Astronomy, University of Glasgow, Glasgow, U.K.

H. Brückmann[17], G. Gloth, U. Holm, H. Kammerlocher, B. Krebs, T. Neumann, K. Wick
Hamburg University, I. Institute of Exp. Physics, Hamburg, Federal Republic of Germany

A. Fürtjes, W. Kröger, E. Lohrmann, J. Milewski[11], M. Nakahata, N. Pavel, G. Poelz, A. Seidman[18], W. Schott, J. Terron[13], B.H. Wiik, F. Zetsche
Hamburg University, II. Institute of Exp. Physics, Hamburg, Federal Republic of Germany

T.C. Bacon, I. Butterworth, C. Markou, D. McQuillan, D.B. Miller, M.M. Mobayyen, A. Prinias, A. Vorvolakos
Imperial College London, High Energy Nuclear Physics Group, London, U.K.

T. Bienz, H. Kreutzmann, U. Mallik, E. McCliment, M. Roco, M.Z. Wang
University of Iowa, Physics and Astronomy Dept., Iowa City, USA

P. Cloth, D. Filges
Forschungszentrum Jülich, Institut für Kernphysik, Jülich, Federal Republic of Germany

L. Chen, R. Imlay, S. Kartik, H.-J. Kim, R.R. McNeil, W. Metcalf
Louisiana State University, Dept. of Physics and Astronomy, Baton Rouge, LA, USA

F. Barreiro[19], G. Cases, L. Hervás[20], L. Labarga[20], J. del Peso, J.F. de Trocóniz[21]
Univer. Autónoma Madrid, Depto de Física Teórica, Madrid, Spain

F. Ikraiam, J.K. Mayer, G.R. Smith
University of Manitoba, Dept. of Physics, Winnipeg, Manitoba, Canada

F. Corriveau, D.J. Gilkinson, D.S. Hanna[4], J. Hartmann, L.W. Hung, J.N. Lim, R. Meijer Drees, J.W. Mitchell, P.M. Patel, L.E. Sinclair, D.G. Stairs, R. Ullmann
McGill University, Dept. of Physics, Montreal, Quebec, Canada

G.L. Bashindzhagyan, P.F. Ermolov, L.K. Gladilin, Y.A. Golubkov, V.A. Kuzmin, E.N. Kuznetsov, A.A. Savin, A.G. Voronin, N.P. Zotov
Moscow State University, Institute of Nuclear Pysics, Moscow, Russia

S. Bentvelsen, M. Botje, A. Dake, J. Engelen, P. de Jong, M. de Kamps, P. Kooijman, A. Kruse, H. van der Lugt, V. O'Dell, A. Tenner, H. Tiecke, H. Uijterwaal[22], M. Vreeswijk, L. Wiggers, E. de Wolf, R. van Woudenberg, R. Yoshida
NIKHEF-Amsterdam, Netherlands

B. Bylsma, L.S. Durkin, K. Honscheid, C. Li, T.Y. Ling, K.W. McLean, W.N. Murray, S.K. Park[23], T.A. Romanowski[24], R. Seidlein
Ohio State University, Physics Department, Columbus, Ohio, USA

G.A. Blair, A. Byrne, R.J. Cashmore, A.M. Cooper-Sarkar, R.C.E. Devenish, D.M. Gingrich[25], P.M. Hallam-Baker[6], N. Harnew, T. Khatri, K.R. Long, P. Luffman, I. McArthur, P. Morawitz, J. Nash, S.J.P. Smith[26], N.C. Roocroft, F.F. Wilson
Department of Physics, University of Oxford, Oxford, U.K.

G. Abbiendi, R. Brugnera, R. Carlin, F. Dal Corso, M. De Giorgi, U. Dosselli, F. Gasparini, S. Limentani, M. Morandin, M. Posocco, L. Stanco, R. Stroili, C. Voci
Dipartimento di Fisica dell' Universita and INFN, Padova, Italy

J.M. Butterworth, J. Bulmahn, G. Feild, B.Y. Oh[27], J. Whitmore[28]
Pennsylvania State University, Dept. of Physics, University Park, PA, USA

U. Contino, G. D'Agostini, M. Guida[29], M. Iori, S.M. Mari, G. Marini, M. Mattioli, A. Nigro
Dipartimento di Fisica, Univ. 'La Sapienza' and INFN, Rome, Italy

J.C. Hart, N.A. McCubbin, K. Prytz, T.P. Shah, T.L. Short
Rutherford Appleton Laboratory, Chilton, Didcot, Oxon, U.K.

E. Barberis, N. Cartiglia, C. Heusch, B. Hubbard, J. Leslie, W. Lockman, K. O'Shaughnessy, H.F. Sadrozinski, A. Seiden
University of California, Santa Cruz, CA, USA

E. Badura, J. Biltzinger, H. Chaves, M. Rost, R.J. Seifert, A.H. Walenta, W. Weihs, G. Zech
Fachbereich Physik der Universität-Gesamthochschule Siegen, Federal Republic of Germany

S. Dagan[30], A. Levy, D. Zer-Zion
School of Physics, Tel-Aviv University, Tel Aviv, Israel

T. Hasegawa, M. Hazumi, T. Ishii, S. Kasai[31], M. Kuze, Y. Nagasawa, M. Nakao, H. Okuno, K. Tokushuku, T. Watanabe, S. Yamada
Institute for Nuclear Study, University of Tokyo, Tokyo, Japan

M. Chiba, R. Hamatsu, T. Hirose, S. Kitamura, S. Nagayama, Y. Nakamitsu
Tokyo Metropolitan University, Dept. of Physics, Tokyo, Japan

R. Cirio, M. Costa, M.I. Ferrero, L. Lamberti, S. Maselli, C. Peroni, A. Solano, A. Staiano
Universita di Torino, Dipartimento di Fisica Sperimentale and INFN, Torino, Italy

M. Dardo
Facultá di Scienze, University of Torino, Alessandria, and INFN-Sezione di Torino, Torino, Italy

D.C. Bailey, D. Bandyopadhyay, F. Benard, S. Bhadra, M. Brkic, B.D. Burow, F.S. Chlebana, M.B. Crombie, G.F. Hartner, G.M. Levman, J.F. Martin, R.S. Orr, J.D. Prentice, C.R. Sampson, G.G. Stairs, R.J. Teuscher, T.-S. Yoon
University of Toronto, Dept. of Physics, Toronto, Ont., Canada

F.W. Bullock, C.D. Catterall, J.C. Giddings, T.W. Jones, A.M. Khan, J.B. Lane, P.L. Makkar, D. Shaw, J. Shulman
University College London, Physics and Astronomy Dept., London, U.K.

K. Blankenship, B.B. Gibaut, J. Kochocki, B. Lu, L.W. Mo
Virginia Polytechnic Inst. and State University, Physics Dept., Blacksburg, VA, USA

K. Charchuła, J. Ciborowski, J. Gajewski, G. Grzelak, M. Kasprzak, M. Krzyżanowski, K. Muchorowski, R.J. Nowak, J.M. Pawlak, A. Stopczyński, T. Tymieniecka, R. Walczak, A.K. Wróblewski, J.A. Zakrzewski, A.F. Żarnecki
Warsaw University, Institute of Experimental Physics, Warsaw, Poland

M. Adamus
Institute for Nuclear Studies, Warsaw, Poland

H. Abramowicz[11], Y. Eisenberg, C. Glasman[32], U. Karshon[30], A. Montag[30], D. Revel, A. Shapira
Weizmann Institute, Nuclear Physics Dept., Rehovot, Israel

C. Foudas, C. Fordham, R.J. Loveless, A. Goussiou, I. Ali, B. Behrens, S. Dasu, D.D. Reeder, W.H. Smith, S. Silverstein
University of Wisconsin, Dept. of Physics, Madison, WI, USA

W.R. Frisken, K.M. Furutani, Y. Iga
York University, Dept. of Physics, North York, Ont., Canada

[1] supported by Worldlab, Lausanne, Switzerland
[2] also at IROE Florence, Italy
[3] now a self-employed consultant
[4] now at DESY as Alexander von Humboldt Fellow
[5] now at CERN
[6] now at DESY
[7] now at IST GmbH, Darmstadt
[8] on leave from Jagellonian University, Cracow
[9] now at Martin & Associates, Hamburg
[10] now at Harry Hoffmann, Fitzbek
[11] on leave from Warsaw University, Warsaw
[12] now at Lufthansa, Frankfurt
[13] supported by the European Community
[14] now at Integrata, Frankfurt
[15] on leave from FERMILAB
[16] now at Blohm & Voss, Hamburg
[17] deceased
[18] on leave from Tel Aviv, University supported by DFG
[19] on leave of absence at DESY, supported by DGICYT
[20] partially supported by Comunidad Autónoma de Madrid, Spain
[21] supported by Fundación Banco Exterior
[22] now at SSC, Dallas
[23] now at Korea University, Seoul
[24] now at Department of Energy, Washington
[25] now at Centre for Subatomic Research, Univ.of Alberta, Canada and TRIUMF, Vancouver, Canada
[26] now with McKinsey Consultants, Sidney, Australia
[27] on leave and supported by DESY 1992-93
[28] on leave and supported by DESY 1991-92
[29] permanent address Dip. di Fisica, Univ. di Salerno, Italy
[30] supported by the MINERVA Gesellschaft für Forschung GmbH
[31] now at Hiroshima National College of Maritime Technology
[32] supported by the DAAD - Deutscher akademischer Austauschdienst

1 Introduction

In lowest order lepton-proton neutral-current deep-inelastic scattering (DIS), the transverse momentum of the scattered electron is balanced by a single jet associated with the struck quark, the proton remnant carrying relatively little transverse momentum. Higher order QCD processes modify this picture. In particular, a hard gluon can be radiated from the struck quark (QCD Compton scattering, QCDC), or a gluon from the proton can interact with the exchanged boson giving rise to quark-antiquark pair production (Boson Gluon Fusion, BGF), as illustrated in Fig. 1 [1-4]. One consequence of these higher order processes is the broadening of the transverse momentum distribution of the particles with respect to the exchanged boson direction, as observed in previous experiments [5]. Recently, the production of jets has been reported in a fixed-target muon experiment at center-of-mass energies up to $\sim$ 30 GeV [6]. With the large increase in center-of-mass energy available at the HERA *ep* collider (295 GeV) clear multijet events should become visible [4].

In this paper we present evidence for events with two or more jets (in addition to the proton remnant) in deep inelastic, neutral current interactions. The events have $Q^2 > 4$ GeV^2, Q^2 being the negative square of the four momentum transfer between electron and proton. The data were collected with the ZEUS experiment in autumn 1992.

2 Experimental setup and data taking

The ZEUS detector is a multipurpose magnetic-detector operating at the HERA storage ring at DESY. Descriptions of the detector, trigger and the data acquisition system were given in previous publications [7-9]. Here we discuss only the parts relevant to this analysis.

Charged particles are reconstructed by the central tracking detector which surrounds the beam pipe and is operated in a magnetic field of 1.43 T, provided by a thin superconducting coil. The chamber consists of 72 cylindrical drift-chamber layers, organised into 9 'superlayers' [10]. Only the inner three axial superlayers were instrumented for this data taking period using a z-by-timing readout [11] with single wire resolutions of $\sigma_z = 4$ cm and $\sigma_{r\phi} = 1$ mm (the ZEUS coordinate system is right handed with the z axis pointing in the direction of the proton beam, hereafter referred to as forward). The tracking information was used to reconstruct the vertex position along the z direction.

The solenoid is surrounded by a high resolution calorimeter divided into three parts, forward (FCAL), barrel (BCAL) and rear (RCAL). The calorimeter is constructed with alternating layers of depleted uranium and scintillator with one sampling every radiation length. The calorimeter is longitudinally segmented into electromagnetic (EMC) and hadronic (HAC) sections subdivided into cells which are read out on either side via wavelength shifter bars and photomultipliers. Under test beam conditions, the calorimeter has shown equal response to incident electrons and hadrons. The energy resolution was found to be $\sigma(E)/E = 0.18/\sqrt{E}$ (E in GeV) for electrons and $\sigma(E)/E = 0.35/\sqrt{E}$ for hadrons [12,13]. To measure the luminosity as well as to tag the scattered electron from very small Q^2 processes, two lead-scintillator electromagnetic calorimeters are installed in the HERA tunnel [14].

The data were collected with a three-level trigger. For the first-level trigger the calorimeter cells were grouped into trigger towers, each approximately 20 cm × 40 cm in transverse area. A first-level trigger was issued whenever the energy deposited in any of the EMC towers or any of the FCAL HAC towers exceeded a programmable threshold [9]. Time information from beam-monitor counters (C5) was used at the first trigger level to reject beam-gas events. The excellent time resolution of the calorimeter signals [12,15] allowed further beam-gas rejection at the second and third trigger levels. The trigger acceptance for the hard scattering events discussed in this paper was greater than 99%.

During 1992, HERA operated with beam energies of 26.7 GeV for the electrons and 820 GeV for protons. In both beams, typical currents of 1-3 mA were stored, distributed over 10 bunches; only nine bunches were used for ep collisions. In addition, one electron and one proton bunch circulated without colliding with a respective proton or electron bunch. These unpaired bunches allowed the study of various backgrounds. The total integrated luminosity was 27 nb^{-1} and about 4 million triggers were collected.

3 Data selection

The off-line data selection proceeded in two steps. First, by selecting events with an EMC trigger, the data sample was reduced from four million triggered events to about 260000 events, with negligible loss of DIS events [9]. In a second step, cosmic rays, beam halo muons and false triggers resulting from an electrical discharge in a single photomultiplier were rejected. Moreover, a more precise determination of the timing in both the C5 counters and the calorimeter allowed a further rejection of beam-related backgrounds. In particular, the time associated with the scattered electron detected in the RCAL was measured with an r.m.s. resolution of 0.5 nsec.

Events were selected with electron candidates of energy larger than 5 GeV, by using the pattern of energy deposits in the calorimeter. The efficiency for identifying scattered electrons was in excess of 98% according to Monte Carlo calculations. From the electron candidates, an estimate of Bjorken y was calculated using the relation:

$$y_e = 1 - \frac{E'_e}{E_e} \frac{1 - \cos\theta'_e}{2} \qquad (1)$$

where θ'_e (E'_e) denotes the polar angle (energy) of the scattered electron and E_e is the energy of the incident electron.

The following requirements were applied to this sample:

- Energy in the FCAL greater than 1 GeV to reduce the background from interactions of the electron beam with the residual gas.
- $\delta = \sum_i E_i\,(1 - \cos\theta_i) \geq 35$ GeV [9], where E_i is the energy measured in the calorimeter cell i with polar angle θ_i. The sum runs over calorimeter cells above the thresholds of 60 MeV (110 MeV) for the EMC (HAC) sections.
- $y_e \leq 0.7$

- In order to ensure a satisfactory reconstruction of the kinematical variables, the estimated Bjorken y obtained from the hadronic system (y_{JB}) [16] was required to satisfy $y_{JB} = \frac{1}{2E_e} \sum_i E_i\,(1 - \cos\theta_i) \geq 0.02$ [9]. Here the sum excludes those calorimeter cells associated with the scattered electron.
- $Q^2 > 4$ GeV^2, where Q^2 was determined with the double-angle method [9,17]. This method uses the angle of the scattered electron and an angle that characterizes the direction of the final hadronic system. Both angles were determined from the calorimeter measurements.

The requirements on y_e and δ were applied in order to reduce the background from photoproduction events in which final state photons or hadrons were misidentified as electrons. These cuts were chosen after detailed Monte Carlo studies for both DIS and photoproduction events [8]. They also remove DIS events with hard initial state radiation. A total of 3808 events passed these cuts.

A sample of these events was visually examined by three independent groups of physicists and found to be free of cosmic rays and halo muons. Moreover, in the 3808 event sample, no event was found in either an unpaired electron or proton bunch.

The analysis was performed using the calorimeter data, i.e., the deposited energies and positions of the calorimeter cells, as well as reconstructed "condensates" [18]. Condensates are contiguous energy deposits in the calorimeter above 100 MeV (200 MeV) in the electromagnetic (hadronic) sections. Monte Carlo studies show that for polar angles above 9° the condensate multiplicity agrees with that of the final state particles to 90%. In addition about 80% of the generated stable particles are associated with only one condensate. At smaller angles the number of reconstructed condensates is many times smaller than the number of generated particles. In the analysis condensates are treated as massless particles.

In order to select multihadronic final states, the number of condensates with polar angles above 9° was required to be larger than four and the total transverse energy, including that of the electron, was required to be larger than 3.5 GeV. These cuts were designed to ensure significant hadronic activity away from the beam pipe. This sample contained 3274 events, and for approximately 95% of these events, primary event vertices were reconstructed. The vertex distribution has an r.m.s. of 26 cm in z. This efficiency is in agreement with Monte Carlo studies of the vertex reconstruction, and the width is consistent with the length of the proton beam bunch.

The photoproduction background in the sample of 3274 events was estimated to be about 1-2%, based on the number of events with an electron detected in the luminosity monitor, and in agreement with Monte Carlo estimates.

4 The Monte Carlo simulation

The Monte Carlo program LEPTO 6.1 [19] was used to model the expected hadronic final states. In this generator, the kinematic variables Q^2 and x are chosen according to the electroweak inclusive cross section for deep inelastic ep scattering, and several parameterizations

of the parton densities are available. Electroweak radiative corrections have not been taken into account, but the selection cuts were tuned to minimize their effect.

For the simulation of the partonic final state, several options are offered in this program. QCD processes to $O(\alpha_s)$ can be included according to exact first order matrix elements (ME). QCD processes including higher order contributions can also be simulated in the leading logarithm approximation (i.e. parton shower approach, PS). This approach is subject to uncertainties in the shower scale, i.e. in the maximum parton off-shellness with two extreme choices being given by Q^2 and W^2 (W being the mass of the hadronic system). A third option, which is used in this study, is a combination of these two approaches (ME+PS), where the first order emission of partons is calculated by the ME contribution and higher order emissions are included through the parton shower. The probabilities for all partonic subprocesses are matched to avoid double counting.

For some comparisons we have also used a "Quark Parton Model" (QPM) Monte Carlo generator based on LEPTO (ME) with the matrix elements for $O(\alpha_s)$ corrections switched off, but with the parton densities keeping their Q^2 dependence.

The fragmentation into hadrons was performed with the Lund string hadronization model [20] as implemented in JETSET 7.3 [21]. The default fragmentation parameters of JETSET, tuned in studies of jets from Z^o decays at LEP [22], have been used. The parton densities in the proton were described with the parameterizations MTB1 [23] or MRSD0 [24].

The detector simulation is based on the general purpose program GEANT 3.13 [25]. The description of the responses of the various detector components was tuned to reproduce test data. Generated event samples were processed with the trigger and detector simulation and the offline data reconstruction procedure.

5 General characteristics of the event sample

In analysing the events, the kinematical variables, Q^2, Bjorken x and W^2, were calculated using the double angle method. The selected events have $x \geq 10^{-4}$. The W distribution, shown in Fig. 2a for the 3808 event sample, spans the range from approximately 30 GeV to 280 GeV, a value close to the kinematical limit; the mean value is $\sim$ 110 GeV. The Monte Carlo predictions exhibit similar features. It is noted that the data in this and subsequent distributions are not corrected for energy loss in uninstrumented regions of the detector, resolution smearing and other detector effects.

The distribution in the total observed transverse energy (E_T) of the hadronic system, shown in Fig. 2b, exhibits a steep fall-off, with a mean value of $\sim$ 5 GeV and a tail which extends up to 40 GeV. The LEPTO (ME+PS) Monte Carlo calculations describes the distribution reasonably well, in particular its high energy tail. The much narrower QPM expectation fails to reproduce the data.

To investigate further the multihadronic final state, an analysis was done in the γ^*p center-of-mass frame. The four-momentum of the exchanged boson (γ^*) was determined from the double angle method. Condensates were used in this analysis in order to study

observables related to individual particles. After removing condensates with polar angles below 9° in the laboratory, an artificial condensate was introduced that enforced energy-momentum conservation. Monte Carlo studies show that the energy and direction of this pseudo-condensate follow closely that of the generated proton remnant. After removing the scattered electron, all remaining condensates, assumed to correspond to massless particles, were boosted to the γ^*p center-of-mass frame. In the QPM the final state would consist, in this frame, of the struck quark travelling close to the direction given by the exchanged boson, while the proton remnant travels in the opposite direction.

The sphericity tensor [26] was then calculated from the observed condensates. Fig. 2c shows the distribution of the transverse momentum square of the condensates with respect to the sphericity axis. The histograms show the Monte Carlo expectations. The data are restricted to the hemisphere around the exchanged photon direction, which should contain the struck quark, and where one expects the gluon radiation effects to be most visible. The distribution is clearly broader than the QPM expectations; the tail extends up to $\sim$ 20 GeV^2 while the QPM predicts no event above 5 GeV^2. Here again the Monte Carlo distribution, including higher order QCD corrections (ME+PS), agrees well with the data.

The transverse momentum distribution discussed above is insensitive to uncertainties in both the scattered electron measurement at small angles and in the reconstruction of the vertex position along the beam direction. Furthermore, due to the cuts in δ and y_e, the effect of electroweak radiative corrections on the transverse momentum distribution is also small.

6 Jet analysis

A search was carried out for two or more jets (in addition to the proton remnant) in the data [27], using a jet finding algorithm in pseudorapidity [1] (η)- azimuth (ϕ) space based on the "Snowmass convention" [28]. The cone radius $R = (\Delta\phi^2 + \Delta\eta^2)^{\frac{1}{2}}$ in the algorithm was set to 1 unit. Calorimeter cells with electromagnetic (hadronic) energy below 60 MeV (110 MeV) were excluded. In order to ensure that the results were not biased by fragments from the proton remnant, cells with polar angles smaller than 9° in the laboratory frame, i.e. $\eta_{cell} > 2.5$, were also excluded. In addition, those calorimeter cells associated with the scattered electron were removed when performing the jet search. Preclusters were formed around cells with transverse energy larger than 0.3 GeV, and the final clusters were called jets if their transverse energy was larger than 4 GeV and $\eta_{jet} \leq 2$, i.e. polar angles larger than 15°.

With the above algorithm, 2502 (76%), 662 (20%), 95(2.9%) and 15(0.5%) events belonging to the zero-, one-, two-, and three-jet categories were found. The jet count includes neither the proton remnant nor the electron. The fact that most of the events have no identified jet is a consequence of the transverse energy cut and the pseudorapidity requirement.

In Fig. 2a we show the distribution (shaded area) of the mass of the hadronic system (W) for two jet events. Note that the mean W value at which two-jet production is seen, 150 GeV, is approximately an order of magnitude larger than those of the highest energy fixed target

[1] Pseudorapidity η is defined in terms of the polar angle θ as $\eta = -\ln \tan\theta/2$.

experiment [5,6]. The transverse energy distribution for the two-jet sample is presented in Fig. 2b (shaded area). Events with higher E_T preferentially have a two-jet structure. For completeness, Fig. 2c shows the contribution (shaded area) of the two-jet sample to the distribution in the square transverse momentum of the condensates with respect to the sphericity axis.

Fig. 3a shows the transverse energy distribution in the (η, ϕ) plane for a one-jet event. This picture illustrates how the transverse momentum is balanced between the scattered electron and the hadronic jet. In this event the proton remnant carries too little transverse energy to be visible. Figs. 3b and 3c show an example each of a two- and a three-jet event, respectively.

The LEPTO (ME+PS) simulation predicts the fractions to be 75%, 22%, 2.8% and 0.2% for the zero-, one-, two- and three-jet categories. These fractions are in reasonable agreement with the experimental data. The agreement between data and Monte Carlo for the jet multiplicities is still preserved when the parameters used in the jet definition are varied, namely $0.8 < R < 1.0$, the jet pseudorapidity cut between 1.5 and 2.5 and the jet transverse energy cut between 3 GeV and 5 GeV.

It should be pointed out that the agreement between data and the Monte Carlo simulation is not fortuitous. The predicted fraction of two- and three-jet events is too large if one uses LEPTO (PS) with the QCD scale set at W^2, while it is too small if the scale is set to Q^2 and zero if the QPM is used. Moreover, LEPTO (ME) predicts no three-jet events although it is able to describe the lower jet multiplicities within the given statistics.

The jet energy profile, which is sensitive to the fragmentation effects, also conforms to expectations. To illustrate this, the transverse energy flow into cells within a cone of radius $R = 2$ around the jet axis was computed. Figs. 3d and 3e show a comparison between data and Monte Carlo simulation for the two- and three-jet samples. The two variables entering in the R definition, i.e. the pseudorapidity $(\Delta\eta)$ and the azimuthal angle $(\Delta\phi)$ measured relative to those of the jet, are plotted separately. These distributions together indicate that a cone size of 1 unit is a reasonable choice, and that the agreement with the LEPTO (ME+PS) Monte Carlo prediction is good. The Monte Carlo calculation, based on exact first order matrix elements only, predicts a jet profile that is somewhat narrower than is observed.

Fig. 4 illustrates some characteristics of the two-jet events compared with Monte Carlo expectations. The comparison is made for the two parameterizations of the parton densities, MTB1 and MRSD0. The jet transverse energy (E_T^{jet}) is shown in Figs. 4a and 4b together with (ME+PS) expectations. The contributions from first order processes only (QCDC and BGF) are also shown. The jet pseudorapidity distribution is presented in Fig. 4c. The difference in azimuth between the two jets is shown in Fig. 4d. A peak near 180° is observed, indicating that the two-jet sample is dominated by back-to-back production in the transverse plane. This is expected since most of the events are at relatively low Q^2 so that the transverse momentum of the electron is small compared to that of the jets. All distributions are in reasonable accord with the Monte Carlo expectations.

Figs. 5a and 5b show the correlation between the pseudorapidities of the jets in the two-jet sample and the expectations from LEPTO (ME+PS) with equal statistics. Here η_{max} (η_{min}) is the pseudorapidity of the jet with the larger (smaller) η value. The two-jet sample from

the Monte Carlo events populates the same region of the (Q^2, x) plane as the data, as seen in Figs. 5c and 5d. Clearly the data are dominated by low x, low Q^2 ($x \leq 10^{-2}, Q^2 \leq 100$ GeV^2) values.

Finally, the Monte Carlo modelling can be used to interpret the data in terms of the underlying processes. In the (ME+PS) approach the two-jet events can originate from two sources. One is from first order processes (QCDC and BGF) where the two partons of the final state have large transverse momentum. The other one is from lowest order processes where the matched parton shower has produced a sufficiently high transverse momentum parton in addition to the struck quark. In Figs. 4a and 4b the predicted contributions originating only from these first order processes are shown separately as the dashed histograms. Thus the E_T^{jet} distribution show that, although at low E_T^{jet} there is a significant contribution from the parton shower associated with the struck quark, the QCDC and BGF become the dominating processes for higher E_T^{jet} values. Of course, the relative contributions from the parton shower and the first order processes predicted by the Monte Carlo model are sensitive to the particular cutoff scheme needed to avoid the singular regions of the matrix elements [19].

7 Summary and conclusions

Multihadronic final states produced in deep inelastic, electron-proton collisions at $Q^2 > 4$ GeV^2 have been investigated for events with center-of-mass energies W between 30 and 280 GeV. The transverse energy and momentum distributions exhibit tails extending to large values which cannot be accounted for by the quark-parton model.

A search for jet production has led to the unambiguous observation of multijet events. Jet rates and the general characteristics of the sample of two-jet events are in agreement with Monte Carlo calculations that include the first order QCD matrix elements plus higher order QCD corrections implemented via parton showers, as presented by the LEPTO (ME+PS) model. The measured jet profiles are also well described by this model. The comparison with the Monte Carlo calculations suggests that two-jet production with large jet transverse energies is dominated by the QCD Compton and BGF processes. These results extend the recent observation of two-jet events reported in [8,29] to a high Q^2 region.

Acknowledgements

The strong support and encouragement by the DESY Directorate Prof. V. Soergel, Drs. H. F. Hoffmann, H. Krech, J. May, D.M. Polter, Profs. P. Söding, G.A. Voss and A. Wagner have been invaluable, as well as the support by Dr. G. Söhngen.

The experiment was made possible by the inventiveness and diligent efforts of the HERA machine group who succeeded in making HERA run in a very short time.

The design, construction, and installation of the ZEUS detector have been made possible by the ingenuity and dedicated efforts of many people from inside DESY and from the home institutes who are not listed here. Their contributions are acknowledged with great appreciation.

We also gratefully acknowledge the support of the DESY computer center.

This work has been supported by the Natural Sciences and Engineering Research Council and the FCAR of Quebec, Canada, by the German Federal Ministry for Research and Technology (BMFT), by the Deutsche Forschungsgemeinschaft (DFG), by the Italian National Institute for Nuclear Physics (INFN), by the Japanese Ministry of Education, Science and Culture (the Monbusho) and its grants for Scientific Research, by the Netherlands Foundation for Research on Matter (FOM), by the Polish Government and Ministry of Education Research Programs, by the Spanish Ministry of Education and Science through funds provided by CICYT, by the UK Science and Engineering Research Council, by the MINERVA Foundation, by the Israel Academy of Science and the Israeli Department of Energy, by the German Israeli Foundation, by the US Department of Energy and by the US National Science Foundation.

References

[1] See for example G. Altarelli, Phys. Rep. C 81 (1982) 1;
F.J. Yndurain, Quantum Chromodynamics, Springer Verlag (1982).

[2] A. Ali et al., Proc. 1987 HERA Workshop, ed. R.D. Peccei (DESY, Hamburg 1988) Vol 1, 395;
S.J. de Jong et al., ibid., Vol 2, 533.

[3] M. Bengtsson et al., Nucl. Phys. B301 (1988) 554;
J. G. Koerner et al., Int. J. Mod. Phys. A4 (1989) 1781 and references therein.

[4] G. Ingelman et al., Proc. 1991 Workshop on Physics at HERA, ed. W. Buchmuller and G. Ingelman (DESY, Hamburg, 1992), Vol. 1, 255.

[5] See for example EMC Collab., J.J. Aubert et al., Phys. Lett. B100 (1981) 433;
M. Arneodo et al., Z. Phys. C36 (1987) 527

[6] E665 Collab., M.R. Adams et al., Phys. Rev. Lett. 69 (1992) 1026.

[7] ZEUS Collab., M. Derrick et al., Phys. Lett. B293 (1992) 465.

[8] ZEUS Collab., M. Derrick et al., Phys. Lett. B297 (1992) 404.

[9] ZEUS Collab., M. Derrick et al., DESY 92-180 (1992), to be published in Phys. Lett. B.

[10] C.B. Brooks et al., Nucl. Instr. and Meth. A283 (1989) 477.

[11] N. Harnew et al., Nucl. Instr. and Meth. A279 (1989) 290;
B. Foster et al., Proc. of 3rd International Conf. on Advanced Technology and Particle Physics, Villa Omo, Como (1992), Oxford Univ. preprint OUNP-92-14, Nucl. Instr. and Meth. (to be published).

[12] A. Andresen et al., Nucl. Instr. and Meth. A309 (1991) 101.

[13] A. Bernstein et al., to be submitted to Nucl. Instr. and Meth.;
U. Mallik et al., Proc. Int. Conf. on Calorimetry in High Energy Physics (Fermilab, 1990).

[14] J. Andruszków et al., DESY 92–066 (1992).

[15] A. Caldwell et al., Nucl. Inst. and Meth. A321 (1992) 352;
A. Caldwell, a presentation at The Int. Conf. on High Energy Physics (Dallas, 1992);
L. Hervas, Thesis, Universidad Autónoma de Madrid (1990), unpublished.

[16] F. Jacquet and A. Blondel, Proc. of the Study for an *ep* Facility for Europe, ed. U. Amaldi, DESY 79/48 (1979) 391.

[17] S. Bentvelsen et al., Proc. 1991 Workshop on Physics at HERA, Vol 1, DESY (1992) 23.

[18] P. de Jong, The Status of the Uranium Calorimeter Reconstruction Software, ZEUS Note 92-019, unpublished.

[19] G. Ingelman, Proc. 1991 Workshop on Physics at HERA, ed. W. Buchmuller and G. Ingelman (DESY, Hamburg, 1992), Vol. 3, 1366;
M. Bengtsson, G. Ingelman and T. Sjöstrand, Nucl. Phys. B301 (1988) 554.

[20] B. Andersson et al., Phys. Rep. C97 (1983) 31.

[21] T. Sjöstrand, Comput. Phys. Commun. 39 (1986) 347;
T. Sjöstrand and M. Bengtsson, Comput. Phys. Commun. 43 (1987) 367.

[22] Th. Hebbeker, Phys. Rep. C217 (1992) 69 and references therein.

[23] J.G. Morfin and W.K. Tung, Z. Phys. C52 (1991) 13.

[24] A. D. Martin, R.G. Roberts, and W.J. Stirling, Durham/RAL preprint, DTP-92-16 and RAL-92-021, to be published in Phys. Rev.

[25] R. Brun et al., GEANT program manual, CERN program library (1992).

[26] J.D. Bjorken and S. Brodsky, Phys. Rev. D1 (1970) 1416.

[27] G. Cases, Ph. D. Thesis, Universidad Autónoma de Madrid (1992), unpublished.

[28] J. Huth et al., Proc. of the 1990 DPF Summer Study on High Energy Physics, Snowmass, Colorado, edited by E.L. Berger (World Scientific, Singapore, 1992) p. 134.

[29] H1 Collab., T. Ahmed et al., Phys. Lett. B297 (1992) 205.

Fig. 1: Feynman diagrams for deep inelastic scattering: (a) Born term, (b) QCD Compton scattering and (c) Boson-Gluon Fusion.

Fig. 2: (a) The distribution of the mass of the hadronic system (W) compared with the LEPTO (ME+PS) Monte Carlo prediction. (b) The transverse energy distribution of the hadronic system in the laboratory frame, measured with respect to the beam direction, compared with predictions of QPM and ME+PS. (c) The square transverse momentum distribution of "condensates" in the $\gamma^* p$ center-of-mass frame, measured with respect to the sphericity axis, together with the predictions of QPM and ME+PS. In each plot the corresponding distribution for the two-jet events is shown as shaded area. The data in this and subsequent figures are not corrected for detector effects.

Fig. 3: Transverse energy distributions of events with jets in the (η, ϕ) plane: (a) one-jet event, (b) two-jet event and (c) three-jet event. (d,e) The profile of jets belonging to the two- and three-jet sample with expectations from the LEPTO 6.1 (ME+PS) and LEPTO (ME) Monte Carlos.

Fig. 4: The distributions of jets for two-jet events measured in the laboratory frame with respect to the beam direction and compared with Monte Carlo expectations calculated using two parameterizations of the parton densities: (a,b) transverse energy (the total and the QCDC+BGF contributions are shown for the Monte Carlo calculations), (c) pseudorapidity and (d) azimuthal angle separation between the two jets.

Fig. 5: Properties of two-jet events: correlation of the jet pseudorapidities for (a) data and (b) Monte Carlo simulations; correlation of x and Q^2 for (c) data and (d) Monte Carlo simulations.

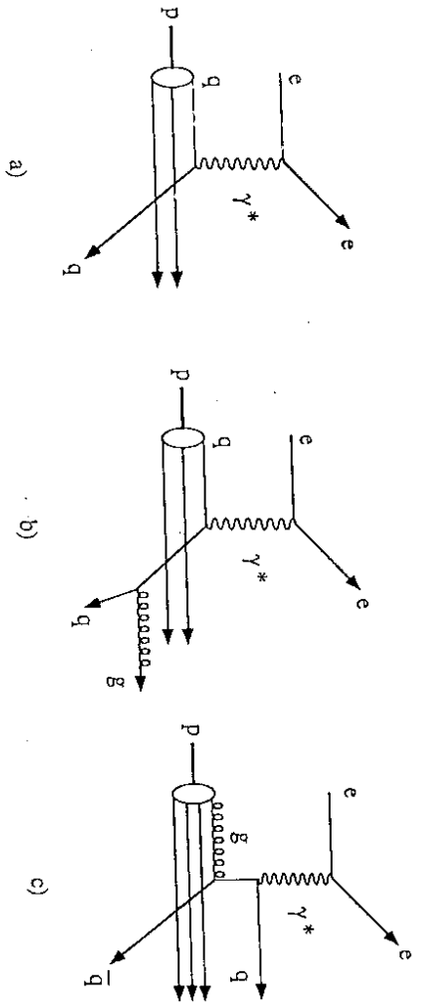

Figure 1.

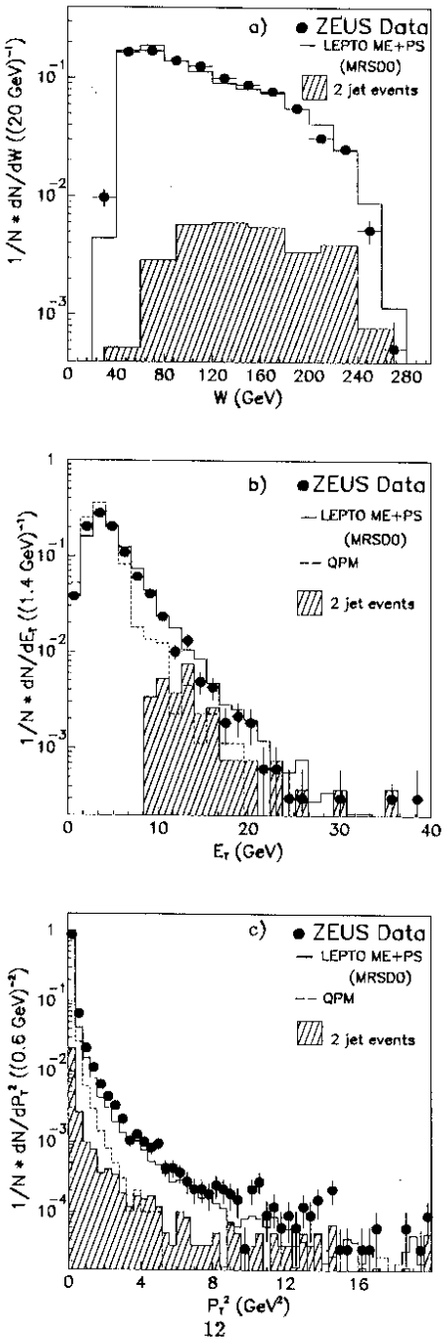

Figure 2.

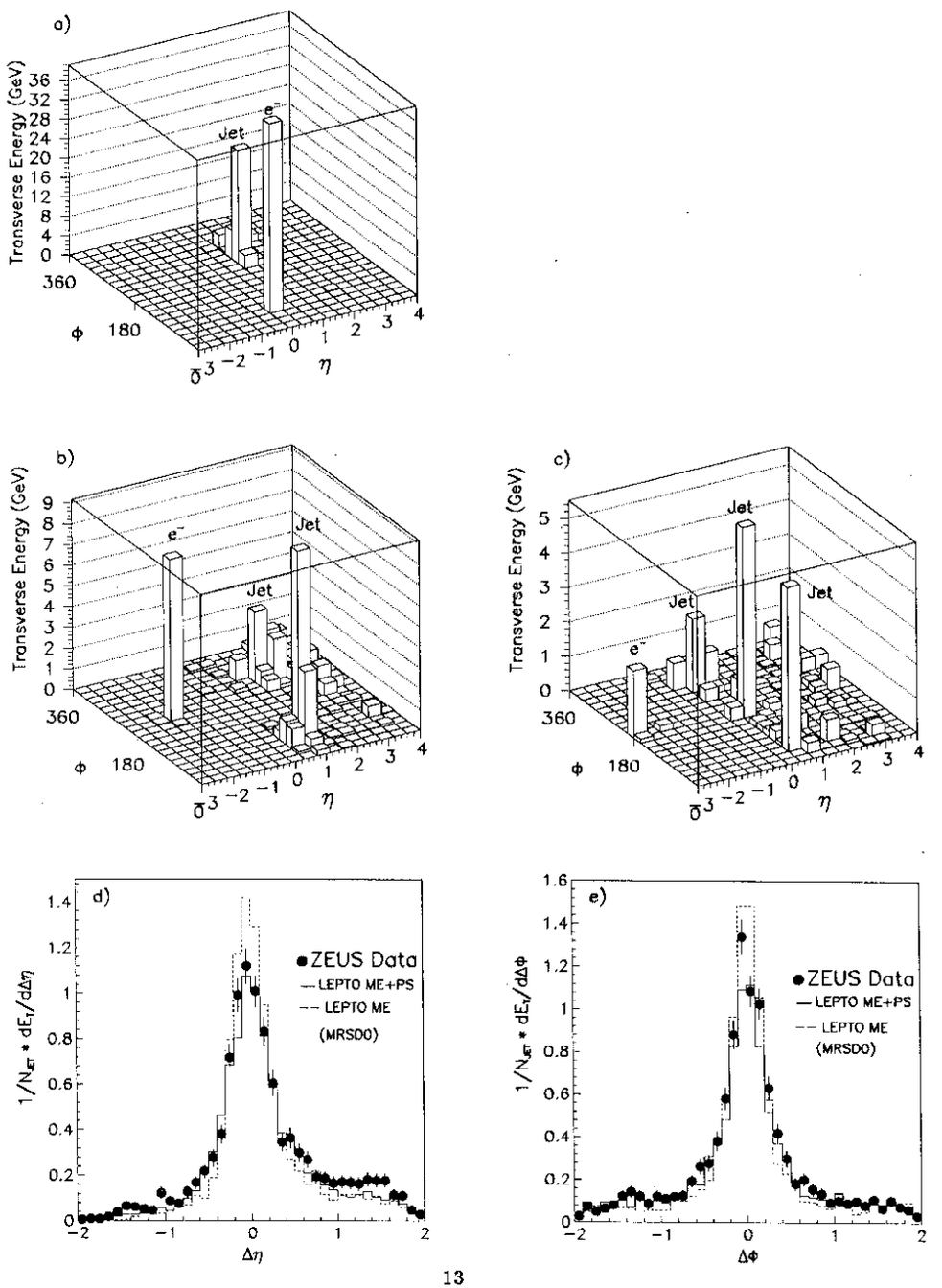

Figure 3.

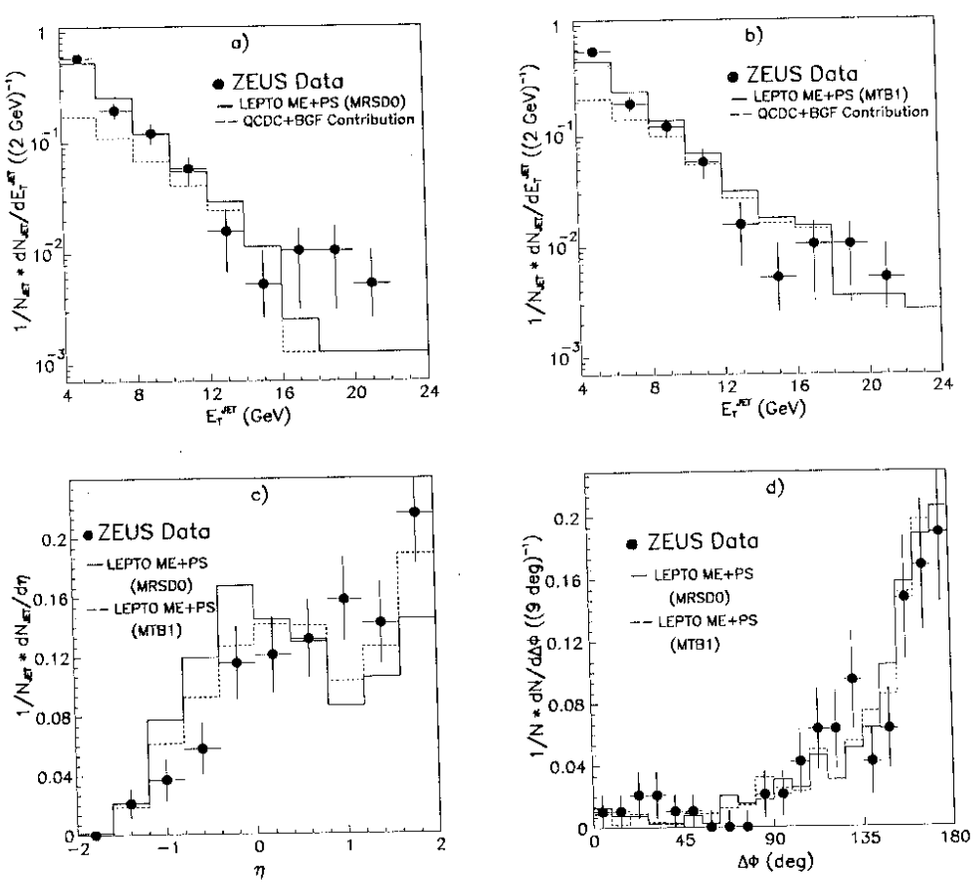

Figure 4.

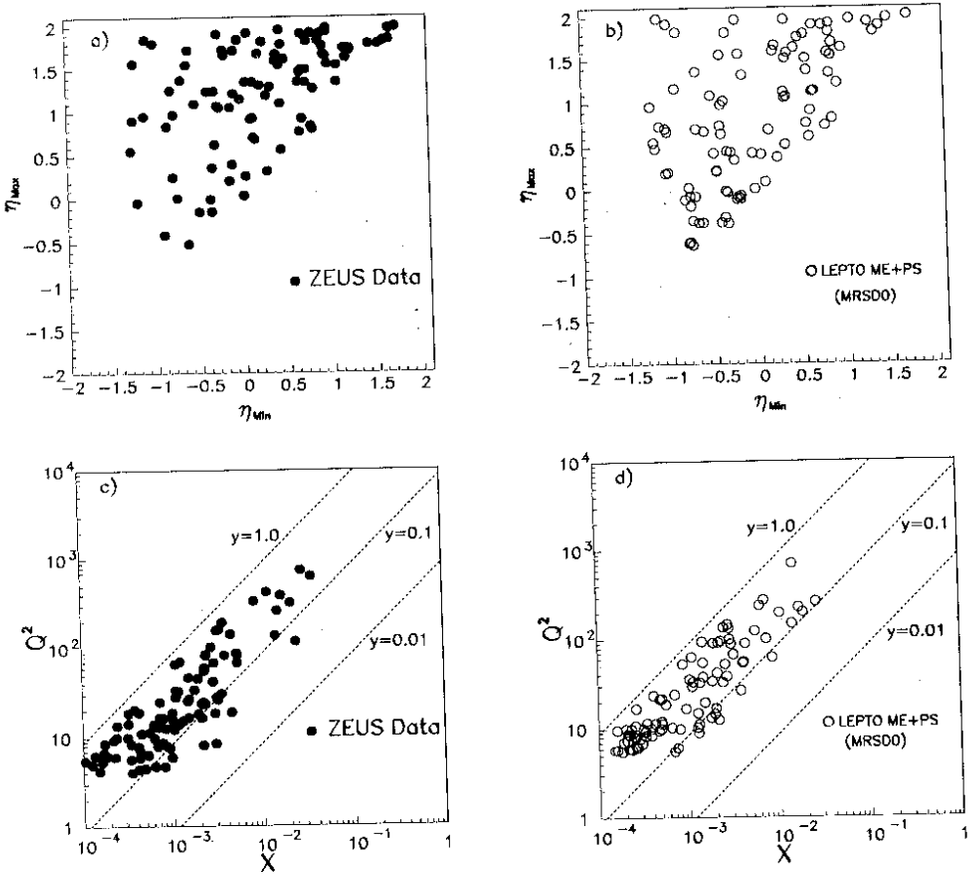

Figure 5.